Oleksandr Povschenko,
Olha Pazdrii

INCREASING SENSITIVITY OF THE ELECTROSTATIC FIELD MILL SENSOR BY DETERMINING ITS OPTIMAL CONFIGURATION

The object of research is the process of measuring the strength of the electrostatic field for a low dynamic range (from 0 to 1 kV/m). This study is aimed at increasing the sensitivity of the sensor of the electrostatic field mill (EF) by determining its optimal geometric configuration, which will reduce the error of measuring the electrostatic field strength.

To establish the actual value of the induced current, a computer model was built and simulation modeling of the EF sensor was carried out. On the basis of the constructed computer model, studies of the EF sensor were carried out to determine the numerical value of the induced current. As a result, it was established that the occurrence of edge effects leads to the appearance of methodological error, which occurs due to the fact that the average induced current is smaller compared to the calculated value. As a result of computer modeling of the EF sensor to determine the value of the optimal number of sectors, it was established that for the proposed design of the EF sensor, the optimal number of sectors is six. It was established that the optimal value of the distance between the sensitive plates and the shielded rotor should be in the range of 2.5–3 mm to ensure the maximum sensitivity of the EF sensor and its safe use.

The determined optimal parameters of the EF geometric configuration will allow to form the necessary requirements for the construction of improved electrostatic field strength meters in a low dynamic range (from 0 to 1 kV/m). A promising direction of application of such devices in production will be the development of an additional system for monitoring the strength of the electrostatic field, which will allow to prevent the occurrence of a dangerous situation.

Keywords: electrostatic fields, electrostatic discharge, electrostatic field mill, measurement, sensor sensitivity.

1. Introduction

In all modern areas of production related to electronics, there are increased regulatory requirements for the conditions of manufacturing, storage and operation of electronic devices [1–3]. This is caused by the vulnerability of electronic components to electrostatic discharge (ESD) [4, 5].

Unpredictable contact between a charged body and an electronic device usually leads to partial or complete damage to the latter, and during its operation can lead to catastrophic consequences. It is difficult to predict the moment of occurrence of an electric discharge, and it is quite difficult to localize the object that accumulated it. Given that all materials are able to accumulate and store electric charge, and the most widespread phenomenon of its formation is the triboelectric effect (the phenomenon of electrification of bodies during friction) [6], there is a need to control the presence of electric charge.

The existing standardized requirements and procedures are aimed at reducing the probability of an electric discharge by creating conditions under which an electric charge cannot exist for a long time [7, 8]. In production or in a laboratory, where there are increased requirements for electrostatic control, a mandatory condition is the creation of so-called electrostatic protected areas (Electrostatic Protected Area (EPA)), which is defined by the standard [9, 10]. Such a zone can be a table, floor, or even the entire room, where the value of the electrostatic field strength is strictly controlled and is below 100 V. All objects located in this zone are grounded and have the same electric potential.

The electric charge accumulated on the surface of the object creates an electrostatic field around itself, the main informative parameter of which is tension. The JEDEC standard defines one of the most widely used simulation test models – the CDM charged device model [1]. The CDM test is used to determine the electrostatic discharge that a device can withstand when the device itself is electrostatically charged and discharged by contact with metal. The ESD threshold voltage is the highest voltage level that does not cause a device failure [11]. Many electronic components are prone to damage from electrostatic discharge at relatively low voltage levels. Many of them are sensitive to a voltage of less than 100 V [4].

With the development of the technology of development of integrated circuits, the size of the internal components of these devices is reduced and they become more sensitive to electrostatic discharge. This is due to an increase in the density of placement of elementary electrical components (transistors) in integrated circuits (ICs). Decreasing

manufacturing technology leads to higher I/O performance and lower contact capacitance, which further increases susceptibility to electrostatic discharge and makes the potential problem even more acute.

In [12], the projected decrease in the sensitivity threshold of microcircuits to the standardized levels of CDM tests for 2020 and subsequent years is shown. Analysis of the collected data shows that a significant reduction in CDM ESD target levels [1] is expected, which in turn requires more accurate measurement for electrostatic field strength monitoring systems.

Many modern components are protected by built-in protection circuits, without which they would be extremely sensitive. But even compliance with all measures cannot fully guarantee the protection of electronic devices against electric shock. To ensure the required level of safety, it is necessary to constantly monitor the strength of the electrostatic field, which will allow not only to record the moment of ESD occurrence, but also to localize its location and establish the source that caused its appearance.

The vast majority of electrostatic field strength meters are designed to determine the strength of electrostatic fields of industrial frequency (50 Hz and higher) [13, 14] or to measure the strength of ultrahigh electrostatic fields (in particular for power lines) [15]. Among the for power line measurement tools considered in [16], the most suitable tool for solving the task of monitoring the strength of the electrostatic field in production is the electrostatic field mill (EF) [17–19].

The main disadvantage of EF is a fairly large measurement error, which is up to 15 % in the range from 0 to 1 kV/m [13]. Such an error is caused by the imperfection of the EF mathematical model, the low sensitivity of the sensor, and the occurrence of amplifier noise during the conversion of current into voltage. Thus, there is a need for research aimed at increasing the sensitivity of existing electrostatic field strength meters in the low dynamic range (from 0 to 1 kV/m) of electrostatic field strength values.

This research is the conduct of research aimed at improving the accuracy of measuring the electrostatic field strength. At the first stage, the authors developed an improved mathematical model of the EF sensor, presented in [20], in order to reduce its methodical error. At the next stage of research, it became necessary to carry out computer simulations of the geometric characteristics of the EF sensor plate to achieve its maximum sensitivity, which will help improve the signal-to-noise ratio, thereby reducing the impact of instrumental error on the measurement result.

The aim of this research is to increase the sensitivity of the EF sensor by determining its optimal geometric configuration, which will allow to reduce the measurement error of the electrostatic field strength. This will make it possible to effectively use EF for tasks of monitoring the strength of the electrostatic field in production.

2. Materials and Methods

The object of research is the process of measuring the strength of the electrostatic field for a low dynamic range (from 0 to 1 kV/m).

2.1. Mathematical model of the electrostatic field mill sensor. An electrostatic field mill, the generalized structure of which is presented in Fig. 1, consists of static sensitive plates and a grounded rotor. Sensitive plates are a circle divided into an even number of sectors, which are electrically connected in two groups A and B through one element. Above them is a shielding plate, which is fixed on a grounded rotor rotating with an angular frequency ω [21]. The movement of the rotor alternately exposes the sensitive plates to the external electric field and shields them, thereby creating a time-varying electric current. The structure and principle of EF operation are described in detail in [20].
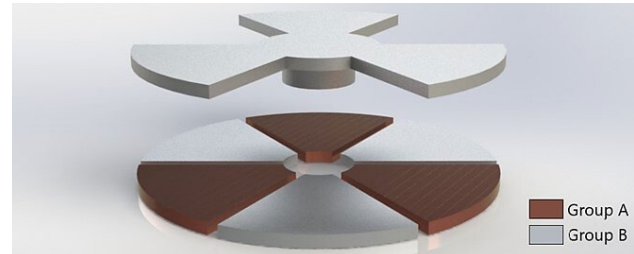
Fig. 1. Generalized view of the sensor plate

The surrounding electric field, which changes at a speed lower than the EF rotation speed, induces a current whose amplitude is directly proportional to the magnitude of the field strength.

Based on the structure of the sensor plate, when its sensitive elements are exposed to an electric field, a charge accumulates on them according to the expression [20]:

$$q(t) = \varepsilon_0 E S(t), \tag{1}$$

where $q(t)$ – the charge accumulated on the cover during time t; E – the background electric field; $S(t)$ – the open area of the plates, variable in time; ε_0 – the dielectric constant of the medium. For a continuous, uniformly rotating rotor, the open area $S(t)$ can be described by a sinusoid, then expression (1) takes the form:

$$q(t) = \varepsilon_0 E S_0 \sin(n\omega t), \tag{2}$$

where S_0 – the nominal area of a set of plates; ω – angular velocity of the rotor; n is the number of sectors of the measuring plate.

Electrostatic field mill can have a different number of measuring plate sectors and a corresponding number of shielding vanes. The effective current induced in the electrodes can be determined by taking the time derivative of equation (2):

$$I(t) = \frac{dq(t)}{dt} = \varepsilon_0 E \frac{dS(t)}{dt}. \tag{3}$$

From which it follows:

$$I(t) = \varepsilon_0 E S_0 n\omega \cos(n\omega t). \tag{4}$$

The area of one group of sensor plates is equal to half the area of the ring formed by the outer radius R of the plate and the inner radius r of the base, by means of which it is attached to the rotor, is found from the ratio:

$$S_0 = \frac{\pi(R^2 - r^2)}{2}. \tag{5}$$

Having written the angular frequency of engine revolutions as $\omega=2\pi f$, let's perform the substitution of relation (5) to expression (4) and after reduction let's obtain the following formula [20]:

$$I(t)=\pi^2(R^2-r^2)\varepsilon_0 Enf\cos(n\omega t). \qquad (6)$$

After analyzing the components of the obtained mathematical model of the EF sensor (6), it can be seen that the magnitude of the current amplitude $I(t)$ in addition to the field strength E is also affected by the area of the sensor plate $\pi(R^2-r^2)$ and the shielding frequency of the plates, which consists of the own frequency of rotation of the shielding plate f and the number of sectors n.

Based on the obtained mathematical model (6), the following approaches exist to increase the sensitivity of the EF sensor:

– increasing the area of the plate;
– increasing the frequency of revolutions;
– increasing the number of sectors of the plate.

Although the presented mathematical model (6) describes well the physics of the processes that take place in the EF sensor, it does not take into account the influence of edge effects. The falling electrostatic field causes distortion at the edges of the shielding plate, which leads to its uneven distribution.

To establish the actual value of the induced current, a computer model was built and simulation modeling of the EF sensor was carried out. Also, on the basis of the built computer model, research was conducted aimed at achieving the maximum sensitivity of the EF sensor. For this, the value of the optimal number of sectors and the distance between the sensitive plates and the shielded EF rotor was determined.

2.2. Simulation model of the electrostatic field mill sensor. COMSOL Multiphysics software was used to build and calculate the numerical model of the EF sensor. It is a finite element analysis, solution, and simulation software for a variety of physics and engineering applications, especially for coupled phenomena or multiphysics.

The computer model of the EF sensor is based on the distribution of the electrostatic field between the sensitive and shielding plates. The structure of the computer model of the EF sensor is shown in Fig. 2.
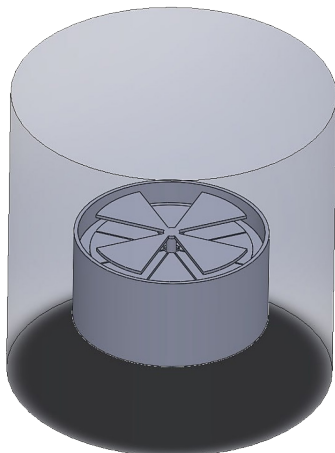

Fig. 2. View of the researched simulation model of the electrostatic field mill sensor

The studied model has 8 open sensitive electrodes and a grounded rotor, where the inner and outer diameters of the blades are 10 mm and 50 mm, respectively. The distance between the sensitive and shielding plates is 3 mm. A cylindrical model of space ($D=200$ mm, $H=200$ mm) filled with air with relative dielectric constant $\varepsilon=1$ was chosen as the medium of electrostatic field propagation. The source of the field strength in the analysis is the upper surface of the cylinder, the voltage on which is set at 100 V. The EF sensor plates are located at a distance of 100 mm from the upper surface of the cylinder, which makes the incident electric field intensity equal to 1 kV/m. The body and rotor of the sensor are grounded and have a potential equal to 0 V.

At the next stage of the research, computer simulation was carried out to establish the actual value of the induced current using the proposed simulation model of the EF sensor.

2.3. Computer modeling of the EF sensor to determine the numerical value of the induced current. On the basis of the constructed EF sensor model, which consists of 8 sectors (Fig. 2), the distribution of the electric field over the sensitive plates during one shielding cycle was constructed. One period of shielding of the plate corresponds to a rotation of the rotor by 45 degrees. Fig. 3 shows the results of modeling the distribution of the electrostatic field intensity depending on the angle of rotation of the rotor. The scale of distribution of electrostatic field strength values in V/m is shown on the right.
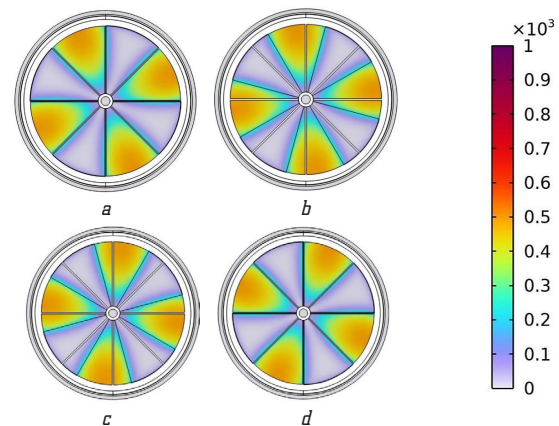

Fig. 3. Distribution of the electrostatic field intensity depending on the angle of rotation of the rotor: a – 0°; b – 15°; c – 30°; d – 45°

The simulation started from the moment of time $t_0=0$, when the sensitive plates were under the shielding plates and were not exposed to the external electric field. At the moment of time t_1, the angle of rotation of the shielding plate was $2\pi/m$, where m – the number of points per one period of rotation of the rotor. Accordingly, the amount of electric charge induced on the sensitive plate can be calculated. The change in the induced electric charge is defined as:

$$\Delta Q=Q_1-Q_0, \qquad (7)$$

where Q_1 – the amplitude value of the induced charge at the moment of full opening of the sensitive plate, and Q_0 – the amplitude value of the induced charge at the moment of full shielding of the sensitive plate.

With an increase in the angle of rotation, the effective area of the sensitive plates, which is exposed to the incident electric field, will increase until it reaches full opening (22.5 degrees). In this case, the value of the induced electric charge Q_1 will be maximum. After passing half of the rotation period, with the subsequent increase in the angle of rotation of the rotor, the value of the induced charge Q_1 will decrease until the sensitive plates are again completely shielded.

2.4. Computer modeling of the EF sensor to determine the value of the optimal number of sectors. The induced current is formed by a periodic change in the effective area of the sensitive plates of the EF sensor within the incident electric field. The faster the area changes, the greater the amplitude of the induced current. When the motor speed is constant, the angular frequency of the induced current signal is equal to $n\omega$, according to the mathematical model (6). Thus, an increase in the number of sectors will lead to an increase in the magnitude of the induced current.

To determine the optimal number of blades of the EF sensor, a computer simulation of the distribution of the electrostatic field between the sensing and shielding plates of the EF was carried out for 9 configurations of the EF with different numbers of sectors. Fig. 4 shows examples of the results of modeling the distribution of electrostatic field strength on EF sensors, which consist of 4, 8, 12, and 18 sectors.
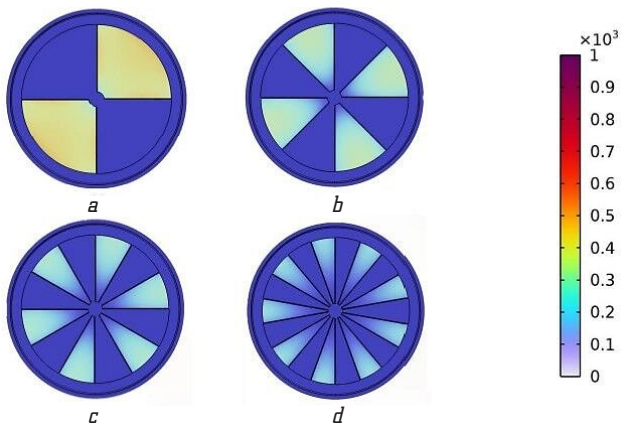

Fig. 4. Distribution of electrostatic field strength on sensors with different number of sectors: a – 4; b – 8; c – 12; d – 18

2.5. Computer modeling of the EF sensor to determine the value of the optimal distance between the sensitive plates and the shielded rotor. To establish the value of the optimal distance between the sensitive plates and the shielded rotor, a computer simulation of the distribution of the electrostatic field between the sensitive and shielding plates of the EF sensor was carried out for 9 different EF configurations.

For modeling, it was decided to use an EF consisting of 8 blades. The sensitive plates were under the direct influence of the electrostatic field. The value of the distance between the plates varied from 2.0 to 6.0 mm in steps of 0.5 mm. Fig. 5 shows examples of the results of modeling the distribution of the electrostatic field depending on the distance between the sensitive and shielding plates for three EF configurations.
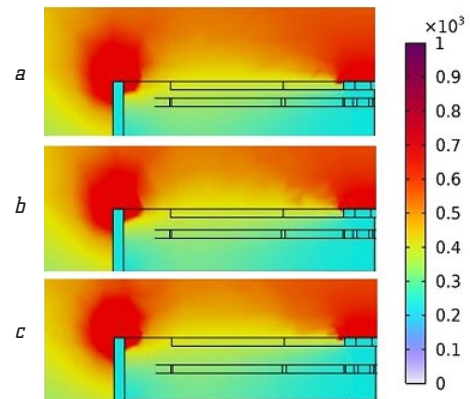

Fig. 5. Distribution of the electrostatic field depending on the distance between the sensitive and shielding plates: a – 2 mm; b – 4 mm; c – 6 mm

As can be seen from Fig. 5, the movement of the sensitive plates does not affect the distribution of the field strength in the device, but when approaching the shielding plate, the magnitude of the field strength acting on them increases.

3. Results and Discussion

As a result of computer modeling of the EF sensor, the following dependences were obtained to determine the numerical value of the induced current: the value of the magnitude of the charge induced on the sensitive plate and the induced current depending on the position of the shielding rotor. Fig. 6 shows the value of the magnitude of the charge induced on the sensitive plate depending on the position of the shielding rotor. From the graph presented, it can be seen that the induced electric charge changes in time non-linearly. This is due to the sinusoidal law of change of the active area of the sensitive plate.

Using the obtained value of the induced charge, the value of the induced current was calculated according to expression (3). The obtained graph of the dependence of the magnitude of the induced electric current on the sensitive plate on the angle of rotation of the EF rotor is shown in Fig. 7.
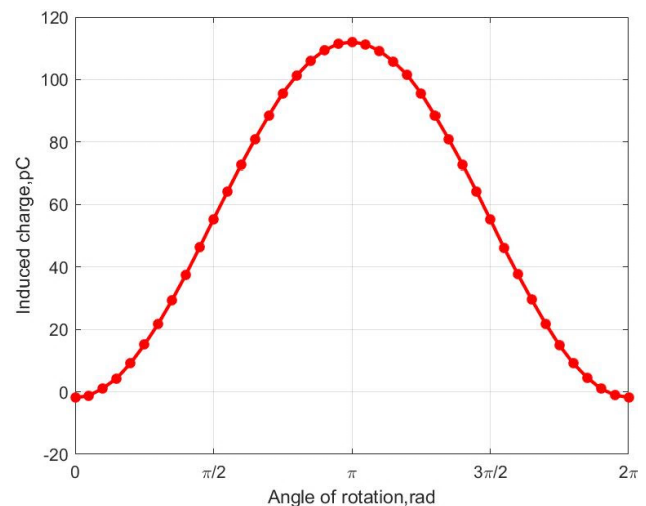

Fig. 6. The magnitude of the induced electric charge on the sensitive plate depending on the angle of rotation of the shielding rotor
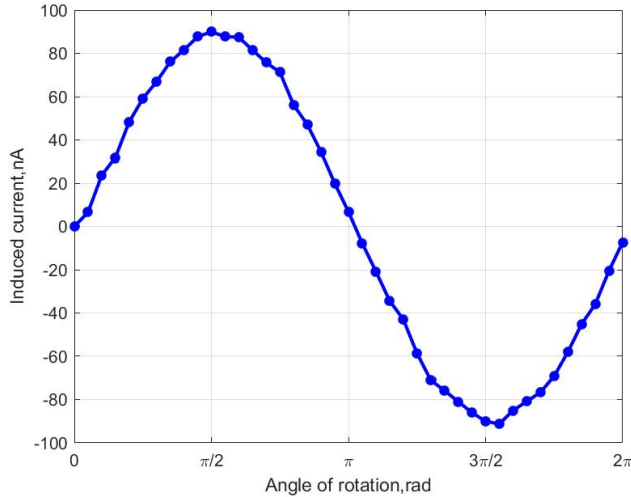
Fig. 7. The magnitude of the induced electric current on the sensitive plate depending on the angle of rotation of the shielding rotor

Based on the mathematical model of the sensor (6), if the sensitive plate is completely shielded, the electric field strength on its surface will be zero, so the magnitude of the induced electric charge Q_0 will also be zero. But, due to the effect of edge effects, when the sensitive plate is completely shielded, some part of the electric field still falls on it and induces a certain electric charge. These effects lead to the occurrence of methodological error in the measurement due to the fact that the average induced current is smaller compared to the calculated value. Due to the occurrence of edge effects, the calculated numerical value of the induced current differs from the current values obtained during simulation.

From the presented results of modeling the distribution of the electrostatic field between the sensitive and shielding plates of the EF for 9 configurations of the EF with different number of sectors (Fig. 4), it can be seen that the magnitude of the electric field strength on the sensitive electrode decreases with an increase in the number of sectors, which is due to the influence of edge effects.

The number of electric charges Q_1 and Q_0 on the sensitive electrode was calculated for 9 EF configurations with different number of sectors (2–18) according to expression (7), and the induced current was calculated according to expression (3).

According to the results of computer modeling, the following dependencies were obtained, the graphs of which are presented in Fig. 8: the value of the magnitude of the charge induced on the sensitive plate and the induced current depending on the number of blades (sectors).

Fig. 8, a shows that the values of the induced charge Q_1 and ΔQ decrease with an increase in the number of blades. This happens because the edge effect affects the distribution of the electric field on the sensitive plates.

An increase in the number of sectors leads to an increase in the influence of edge effects, which in turn reduces the intensity of the electric field. Thus, increasing the sensitivity of the EF sensor due to the increase in sectors has a marginal value. Fig. 8, b shows that the maximum induced current is reached when the number of opening electrodes reaches six.

As a result of computer modeling of the EF sensor to determine the value of the optimal distance between the sensitive plates and the shielded rotor, the dependences of the values of the gap between the plates on the value of the induced charge and the induced current were obtained.

Fig. 9, a shows that as the distance between the sensitive plates and the shielded rotor increases, the value of the induced electric charge Q_1 and the magnitude of the change in the induced electric charge ΔQ decrease. Fig. 9, b shows that the average induction current decreases with an increase in the distance between the plates.
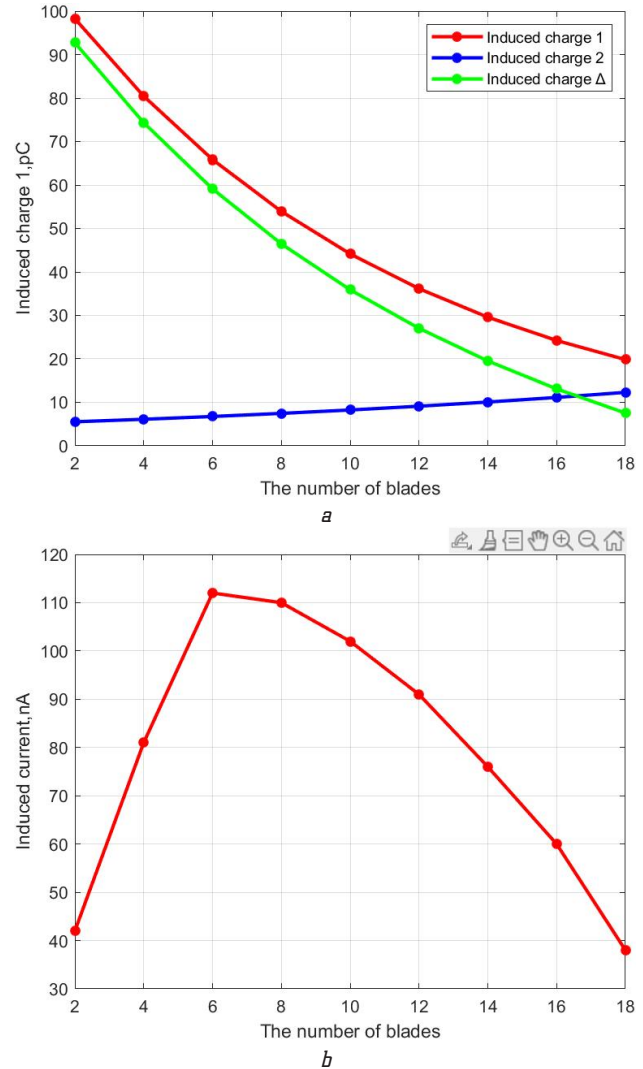

a

b

Fig. 8. The resulting graphs: a – changes in the induced electric charge; b – changes in the induced current

The presented results confirm the hypothesis that the value of the induced current is also affected by the value of the distance between the plates.

Analyzing the graphs obtained, shown in Fig. 9, it can be concluded that the value of the distance between the sensitive plates and the shielded rotor should be as small as possible to increase the sensitivity of the EF sensor. But, in practice, placing sensitive and shielding plates too close to each other can cause an electric discharge between them when condensation forms on the surface of the plates. Therefore, it was assumed that the optimal value of the distance between the EF sensor plates is 2.5–3 mm.

The dependences obtained as a result of computer modeling will make it possible to form the necessary requirements for the construction of an EF sensor in new devices that are focused on measuring the strength of the electrostatic field in a low dynamic range (from 0 to 1 kV/m).
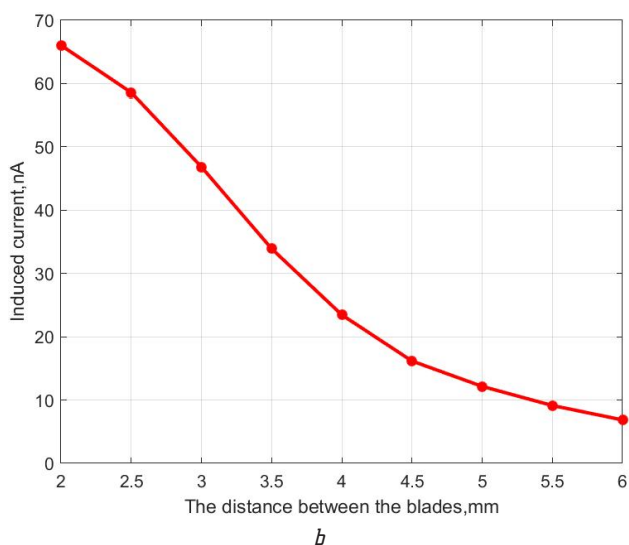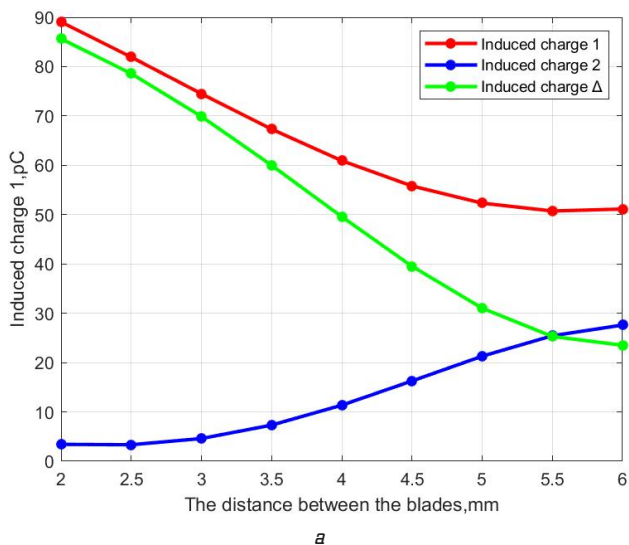
Fig. 9. The resulting graphs: *a* – changes in the induced electric charge;
b – changes in the induced current

The determined optimal parameters of the geometric configuration of the EF, such as the number of sectors and the distance between the sensitive plates and the shielded rotor of the EF for the proposed design of the device, will allow to increase the sensitivity of the EF sensor. This will make it possible to effectively use EF for tasks of monitoring the strength of the electrostatic field in production.

Limitations of the study. The research presented in the work is limited to the use of computer simulations only. For the most part, this limitation is due to the imperfection of the mathematical models used by the software. Measurements using computer models are limited by the grid size of the model, which introduces certain uncertainties in the field distribution. The influence of such factors is difficult to assess, so the obtained values may differ from the experimental ones.

The influence of martial law conditions. The large-scale military aggression of the russian federation against Ukraine, launched on February 24, 2022, caused a number of acute problems in the field of science and innovation. Partially destroyed or damaged research infrastructure, reduction of state and local budget expenditures on education and forced displacement of scientific and scientific-pedagogical workers

from their own homes and places of employment contributed to the loss of scientific potential in the field of scientific research. Along with this, logistical connections became more complicated and production capacity decreased, which directly affected the possibility of mock-up and small-scale production of research models and own devices.

Prospects for further research. Future research will include conducting a physical experiment, developed on the basis of computer modeling of the structure, taking into account the established optimal parameters of the structure of the EF sensor. Research and development of sensitive electrostatic field strength meters can be used in the future to increase the level of protection of electronic devices against electrostatic discharge. Such a device will allow not only to record the moment of ESD occurrence, but also to localize its location.

4. Conclusions

The research presented in the work is aimed at increasing the sensitivity of the EF sensor by determining its optimal geometric configuration.

At the first stage of research, to establish the optimal geometric configuration of the EF sensor, its computer model was built. As a result of the conducted simulation modeling of the EF sensor, the following conclusions can be drawn:

– Although the mathematical model (6) describes well the physics of the processes that take place in the EF sensor, it does not take into account the influence of edge effects. During the computer simulation of the EF sensor to determine the numerical value of the induced current, it has been established that the occurrence of edge effects leads to the appearance of a methodical error, which arises due to the fact that the average induced current is smaller compared to the calculated value.

– As a result of computer modeling of the EF sensor to determine the value of the optimal number of sectors, it has been established that an increase in their number leads to an increase in the influence of edge effects. Thus, increasing the sensitivity of the EF sensor due to the increase in sectors has a marginal value. It has been established that for the proposed design of the EF sensor, the optimal number of sectors is six.

– Analysis of the obtained results of computer modeling of the EF sensor has been shown that the optimal value of the distance between the sensitive plates and the shielded rotor should be in the range of 2.5–3 mm to ensure the maximum sensitivity of the EF sensor and its safe use.

The determined optimal parameters of the EF geometric configuration will allow to form the necessary requirements for the construction of improved electrostatic field strength meters in a low dynamic range (from 0 to 1 kV/m). A promising direction of application of such devices in production will be the development of a monitoring system to increase the level of protection of electronic devices against impact by electrostatic discharge.

Conflict of interest

The authors declare that they have no conflict of interest in relation to this study, including financial, personal, authorship, or any other, that could affect the study and its results presented in this article.

Financing

The study was conducted without financial support.

Data availability

The manuscript has no associated data.

Use of artificial intelligence

The authors confirm that they did not use artificial intelligence technologies when creating the current work.

References

1. *ESDA/JEDEC Joint Standard For Electrostatic Discharge Sensitivity Testing – Charged Device Model (CDM) – Device Level, JS-002-2022. ANSI/ESDA/JEDEC* (2022). Rome, New York.
2. *ESDA/JEDEC Joint Standard For Electrostatic Discharge Sensitivity Testing – Human Body Model (HBM) – Component Level, JS-001-2023. ANSI/ESDA/JEDEC* (2023). Rome, New York.
3. Voldman, S. H. (2021). *ESD Handbook.* John Wiley & Sons, Ltd. doi: https://doi.org/10.1002/9781119233091
4. Smallwood, J. (2023). *A Guide to ESD.* EMC Information Centre. Available at: https://www.nutwooduk.co.uk/archive/old_archive/030923.htm Last accessed: 19.11.2023
5. *Fundamentals of Electrostatic Discharge. Part One – An Introduction to ESD* (2020). EOS/ESD Association, Inc. Available at: https://www.esda.org/esd-overview/esd-fundamentals/part-1-an-introduction-to-esd/ Last accessed: 19.11.2023
6. Pan, S., Zhang, Z. (2018). Fundamental theories and basic principles of triboelectric effect: A review. *Friction, 7 (1)*, 2–17. doi: https://doi.org/10.1007/s40544-018-0217-7
7. Ruffat, F., Caignet, F., Boyer, A., Escudié, F., Mejecaze, G., Puybaret, F. (2022). New measurement method to investigated service life of protection networks exposed to ESD. *Microelectronics Reliability, 138*, 114661. doi: https://doi.org/10.1016/j.microrel.2022.114661
8. Gao, Y., Cai, X., Han, Z., Zeng, C., Xia, R., Tang, Y., Gao, M., Li, B. (2023). Design of compact-diode-SCR with low-trigger voltage for full-chip ESD protection. *Microelectronics Reliability, 140*, 114860. doi: https://doi.org/10.1016/j.microrel.2022.114860
9. *Protection Of Electrical And Electronic Parts, Assemblies And Equipment (Excluding Electrically Initiated Explosive Devices), S20.20-2021, ANSI/ESD* (2021). Rome, New York.
10. *Electrostatics – Part 5-2: Protection of Electronic Devices from Electrostatic Phenomena – User Guide, TR 61340-5-2:2018* (2018). IEC.
11. *ESD Association Advisory for Electrostatic Discharge Terminology – Glossary, ADV1.0-2017* (2017). ESD.
12. Righter, A., Carn, B. (2017). A Look at the New ANSI/ESDA/JEDEC JS-002 CDM Test Standard. *Analog Dialogue, 51 (4),* 11–15. Available at: https://www.analog.com/en/analog-dialogue/articles/a-look-at-the-new-ansi-esda-jedec-js-002-cdm-test-standard.html
13. Ponnle, A. A. (2022). Measurement and Assessment of Exposure to 50 Hz Magnetic Fields from Common Home Electrical Appliances. *European Journal of Engineering and Technology Research, 7 (3),* 119–127. doi: https://doi.org/10.24018/ejeng.2022.7.3.2832
14. Xiao, D., Ma, Q., Xie, Y., Zheng, Q., Zhang, Z. (2018). A Power-Frequency Electric Field Sensor for Portable Measurement. *Sensors, 18 (4),* 1053. doi: https://doi.org/10.3390/s18041053
15. Oltean, M. N., Fagarasan, T., Florea, G., Munteanu, C., Pop, A. (2017). Electromagnetic field measurement on high voltage overhead lines. *2017 12th International Conference on Live Maintenance (ICOLIM).* doi: https://doi.org/10.1109/icolim.2017.7964148
16. Povcshenko, O., Bazhenov, V. (2023). Analysis of modern atmospheric electrostatic field measuring instruments and methods. *Technology Audit and Production Reserves, 4 (1 (72)),* 16–24. doi: https://doi.org/10.15587/2706-5448.2023.285963
17. Swenson, J. A., Beasley, W. H., Byerley, L. G., Bogoev, I. G. (2017). Pat. US 7.256,572 USA. *Electric-field meter having current compensation.* published: 14.08.2007. Available at: https://patents.google.com/patent/US7256572B2/en?oq=US+7.256%2c572
18. Chester, D. S. (1976). Pat. US 4'095'221 USA. *Electrical storm forecast system.* published: 13.07.1976. Available at: https://patents.google.com/patent/US4095221A/en?oq=US+4%27095%27221
19. Wells, T. J., Elliott, R. S. (2005). Pat. US 6'982'549 USA. *Microelectrometer.* published: 05.12.2005. Available at: https://patents.google.com/patent/US6982549B1/en?oq=US+6%27982%27549
20. Bazhenov, V., Povcshenko, O. (2023). Methodological features of calculating errors in the measurement of electrostatic field strength. *Bulletin of Kyiv Polytechnic Institute. Series Instrument Making, 65 (1)*, 65–72. doi: https://doi.org/10.20535/1970.65(1).2023.283358
21. Antunes de Sá, A., Marshall, R., Sousa, A., Viets, A., Deierling, W. (2020). An Array of Low-Cost, High-Speed, Autonomous Electric Field Mills for Thunderstorm Research. *Earth and Space Science, 7 (11).* doi: https://doi.org/10.1029/2020ea001309

✉**Oleksandr Povschenko,** *Postgraduate Student, Department of Informational Measuring Equipment, National Technical University of Ukraine «Igor Sikorsky Kyiv Polytechnic Institute», Kyiv, Ukraine, e-mail: scela2472@gmail.com, ORCID: https://orcid.org/0000-0003-2998-5950*

Olha Pazdrii, *Assistant, Department of Computer-Integrated Optical and Navigation Systems, National Technical University of Ukraine «Igor Sikorsky Kyiv Polytechnic Institute», Kyiv, Ukraine, ORCID: https://orcid.org/0000-0002-8970-5079*

✉*Corresponding author*